MEASUREMENT OF PROTON PROTON ELASTIC SCATTERING IN PURE INITIAL SPIN STATES AT 11.75 GeV/c ☆

K. ABE, R.C. FERNOW, T.A. MULERA, K.M. TERWILLIGER
Randall Laboratory of Physics, University of Michigan, Ann Arbor, Michigan 48104, USA

W. De BOER
Max Planck Institute für Physik, D-8 Munich-40, Germany

A.D. KRISCH *
Niels Bohr Institute, Dk-2100 Copenhagen, Denmark

H.E. MIETTINEN
CERN, CH-1211 Geneva, Switzerland

J.R. O'FALLON
Department of Physics, St. Louis University, St. Louis, Missouri 63103, USA

L.G. RATNER
Accelerator Research Facilities Division, Argonne National Laboratory, Argonne, Illinois 60439, USA

Received 23 April 1976

The elastic cross section for proton proton scattering at 11.75 GeV/c was measured at the Argonne ZGS using a 50% polarized target. In the range $p_\perp^2 = 0.6 \rightarrow 2.2$ (GeV/c)^2 we obtained precise measurements of $d\sigma/dt(ij)$ for the $\uparrow\uparrow$, $\downarrow\downarrow$, and $\uparrow\downarrow$ initial spin states perpendicular to the scattering plane. We confirmed that the asymmetry parameter, A, decreases with energy in the diffraction peak, but is approximately energy-independent at large $p_\perp^2$. We found that the spin correlation parameter c_{nn} acquires rather dramatic structure, and at large $p_\perp^2$ seems to grow with energy.

In recent years the evidence for the importance of spin dependence in high energy strong interactions has been increasing. This spin dependence was first studied successfully using the polarized proton targets at Berkeley [1], CERN [2], and Argonne [3]. During the past few years the ZGS polarized beam has allowed new and even more precise measurements of the elastic spin dependence [4–7]. Recently the polarized beam operated at 11.75 GeV/c allowing the first measurements of pure spin elastic cross sections above 6 GeV/c.

The polarized beam was accelerated to 11.75 GeV/c to avoid extraction near the very strong depolarizing resonance at 12.11 GeV/c [8]. The internal intensity at 11.75 GeV/c was as high as 7×10^9 per 4.0 sec pulse. The extracted beam intensity was as high as 4×10^9 and averaged about 2.5×10^9 per pulse. There was some difficulty with beam depolarization due to limits on the pulsed quadrupole currents necessary to completely jump the last few depolarizing resonances [8]. The average polarization for the entire one month run was about $p_B \approx 47\%$. The ZGS staff [9] partially reduced the depolarization by reducing the vertical beam size; and by the end of the run P_B was averaging about 55%. Further work on the pulsed quadrupoles and beam size will be necessary to maintain a 75% polarization, as at 6 GeV/c.

We scattered the polarized beam from the Michigan-Argonne PPT V polarized proton target [10], which is a close copy of a CERN target [11]. The PPT

☆ Work supported by U.S. Energy Research and Development Administration
* On leave from The University of Michigan.

is maintained at 0.5°K in a magnetic field of 25 Kg and contains beads of propanediol, $C_3H_8O_2$, doped with $K_2Cr_2O_7$ in a flask 4.13 cm long by 2.9 cm in diameter. The free protons in the propanediol are pumped into a polarized state by the 70 GHz microwaves from a carcinotron tube, using the highly polarized Cr electrons. The proton polarization is measured using a 107 MHz NMR system with signal averaging, which is calibrated against the known thermal equilibrium polarization with a ± 3% precision. The target polarization has been as high as P_T = 85%, but the high polarized beam intensity caused radiation damage which reduced the average P_T to about 65%. Maintaining even 65% required annealing the PPT every 3 days to remove some of the radiation damage. Two independent NMR coils with different diameters measured the variation of P_T with transverse position caused by the variation in radiation damage. The small coil was a straight wire along the beam axis; the large coil was a 1.0 cm diameter helix coaxial with the beam axis. With a freshly annealed PPT the measured P_T difference between the two coils was less than 2%; but after several days of irradiation the difference was as large as 7%. We averaged the values of P_T measured by the two coils.

The beam polarization was measured using the high energy polarimeter shown in fig. 1. This was very similar to the polarimeter used in our earlier measurements [4, 6, 7] and was only modified slightly to operate at 11.75 GeV/c. At this energy the asymmetry parameter, A, is only about 5% in the diffraction peak but is much larger at large $P_\perp^2$. Thus we set the polarimeter to simultaneously measure p–p elastic scattering to the left, L, and to the right, R, at $P_\perp^2$ = 1.4 (GeV/c)^2. The beam polarization is given by

$$P_B = \frac{1}{A}\left(\frac{L-R}{L+R}\right). \quad (1)$$

We obtained A at $P_\perp^2$ = 1.4 (GeV/c)^2 by measuring elastic scattering from our downstream polarized target using the FB spectrometer shown in fig. 1 and described later. In this calibration run the beam polarization was ignored and we used the measured polarization of the target to obtain A = 15.83 ± 0.80%. This was combined with a nearby [12] result at $P_\perp^2$ = 1.42 (GeV/c)^2 and 12.33 GeV/c of A = 14.7 ± 2.0% to give for the asymmetry parameter

$$A = 15.7 \pm 0.7\% \quad (2)$$

which we take to be the analyzing power of our polarimeter. We directly showed that the analyzing powers, A, of the polarimeter and the spectrometer were identical by comparing the two simultaneously measured asymmetries during the $P_\perp^2$ = 1.4 (GeV/c)^2

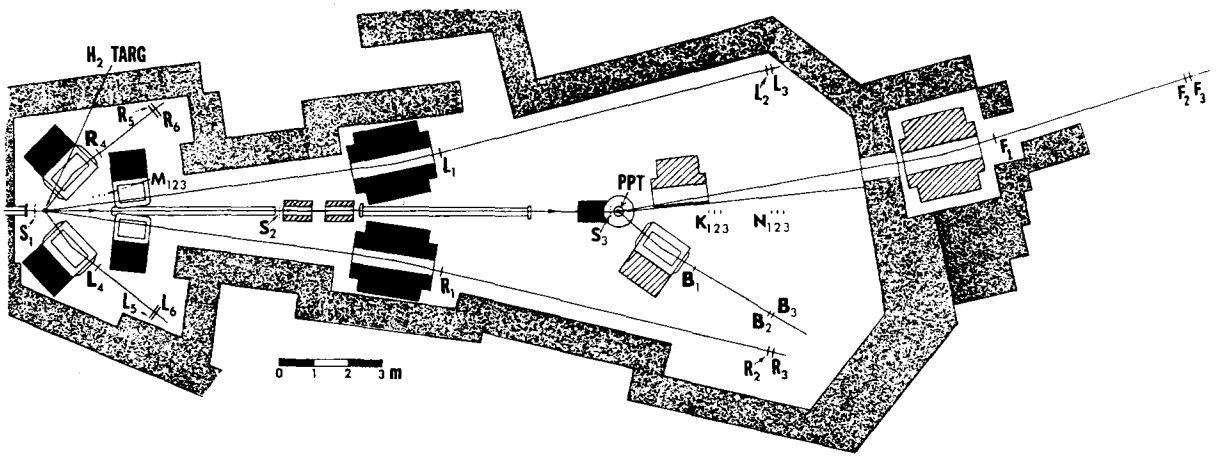

Fig. 1. Layout of the experiment. The polarized beam passes through the H_2 target and its polarization is measured by comparing the number of elastic events seen in the L and R spectrometers of the polarimeter. The beam then scatters in the polarized proton target (PPT) and the elastic events are counted by the F and B counters. The M, N and K counters are intensity monitors, while S_1, S_2, and S_3 monitor the beam position.

calibration run:

$$P_B A \text{ (spectrometer)} = \frac{FB(\uparrow) - FB(\downarrow)}{FB(\uparrow) + FB(\downarrow)} = 7.54 \pm 0.52\%$$
$$P_B A \text{ (polarimeter)} = \frac{L - R}{L + R} = 7.69 \pm 0.19\%. \quad (3)$$

The FB(↑) and FB(↓) are the elastic event rates with the beam spin respectively up and down.

We used the double arm FB spectrometer to measure the differential cross section for the elastic scattering of the polarized beam from the polarized target. This spectrometer measured both the angle and momentum of both the scattered and the recoil protons, using 3 magnets and the 6 scintillation counters $F_1F_2F_3$ and $B_1B_2B_3$ as shown in fig. 1. By varying the currents in the 3 magnets and reversing the PPT magnet we were able to cover the range $P_\perp^2 = 0.6 \rightarrow 2.2$ $(\text{GeV}/c)^2$ by only moving the B counters. The forward scattered proton was defined by the 15 X 13 cm (hor. X vert.) F_3 counter placed about 18.4 m from the PPT. The F_3 momentum bite was $\Delta P/P = \pm 7\%$ while $\Delta\Omega_{lab} \approx 0.57\ 10^{-4}$ sr. The recoil proton was defined by the 5 X 20 cm B_3 counter placed about 5.5 m from the PPT. The B_3 momentum bite was $\Delta P/P = \pm 3\%$ while $\Delta\Omega_{lab} \approx 3.3\ 10^{-4}$ sr. The c.m. angle subtended by F_3 and B_3 each varied considerably as $P_\perp^2$ was changed between 0.6 and 2.2 $(\text{GeV}/c)^2$ due to changes in the Jacobians and in magnetic focusing. Thus sometimes F_3 defined vertically while B_3 defined horizontally and sometimes the opposite occurred. Moreover since the c.m. angles were almost equal, there was insufficient "overmatching" to allow for multiple Coulomb scattering, beam size and divergence, and magnet variation. These effects reduced the "effective" solid angle by as much as 50% with a large uncertainty. We decided to accept this uncertainty and to use other data [13] to normalize our absolute differential cross sections. Thus we obtained a very clean elastic signal by keeping tight angle and momentum constraints on both arms. Recoil magnet curves at $P_\perp^2 = 0.6$, 1.0, 1.4 and 2.2 $(\text{GeV}/c)^2$ indicated that inelastic events and events from non-hydrogen protons were typically less than 3%. The F–B accidentals were continuously monitored and subtracted and were always less than 0.3%.

We monitored the size, position, and angle of the beam at both targets using the segmented wire ion chambers (SWIC's) shown in fig. 1 as S_1, S_2, and S_3. These were maintained by the ZGS staff. The beam size at the PPT was about 10 mm FWHM and the beam was kept centered to about ±0.5 mm. The beam profile indicated that more than 97% of the beam passed through the 29 mm diameter PPT. This reduced possible errors due to variations in the fraction of the beam passing through the PPT caused by beam movement and by changes of the beam size. This error was reduced further by flipping the direction of the beam spin every pulse and reversing the target spin about every 8 hours and then signal averaging away any variations. The remaining uncertainty was normally less than 1% as will be shown later.

We want to obtain the differential elastic cross sections $d\sigma/dt(ij)$ in each initial spin state normal to the scattering plane (i, j = beam, target). We must first calculate the normalized event rate, N_{ij}, from the number of FB(ij) events in each of the 4 initial spin states (↑↑, ↑↓, ↓↑, and ↓↓) using

$$N_{ij} = \frac{FB(ij)}{I_o(ij)}. \quad (4)$$

The quantity $I_o(ij)$ is the number of incident protons which was measured by the N and K monitors which were calibrated during aluminum foil irradiation runs with a 7% normalization uncertainty. Our final results are totally independent of this uncertainty. We then calculated the 4 pure two-spin cross sections from the equations

$$d\sigma/dt(\uparrow\uparrow) = \langle d\sigma/dt\rangle [1 + 2A + C_{nn}]$$
$$d\sigma/dt(\downarrow\downarrow) = \langle d\sigma/dt\rangle [1 - 2A + C_{nn}] \quad (5)$$
$$d\sigma/dt(\uparrow\downarrow) = d\sigma/dt(\downarrow\uparrow) = \langle d\sigma/dt\rangle [1 - C_{nn}]$$

where $\langle d\sigma/dt\rangle$ is the measured [13] spin average cross section. The spin correlation parameter C_{nn} is given by

$$C_{nn} = \frac{N_{\uparrow\uparrow} - N_{\uparrow\downarrow} - N_{\downarrow\uparrow} + N_{\downarrow\downarrow}}{P_B P_T \Sigma N_{ij}} \quad (6)$$

The asymmetry parameter A is obtained by averaging over either the target or beam polarization

$$A_B = \frac{N_{\uparrow\uparrow} + N_{\uparrow\downarrow} - N_{\downarrow\uparrow} - N_{\downarrow\downarrow}}{P_B \Sigma N_{ij}}$$
$$A_T = \frac{N_{\uparrow\uparrow} - N_{\uparrow\downarrow} + N_{\downarrow\uparrow} - N_{\downarrow\downarrow}}{P_T \Sigma N_{ij}} \quad (7)$$

Table 1
List of A, C_{nn}, and $d\sigma/dt(ij)/\langle d\sigma/dt\rangle$ for each $P_\perp^2$ *. The values of A_T and A_B whose equality is a consistency check are also given. The errors in $\sigma(\downarrow\downarrow)$ and $\sigma(\uparrow\uparrow)$ are identical.

$P_\perp^2$ [GeV/c]^2	A_T [%]	A_B [%]	A [%]	C_{nn} [%]	$\frac{d\sigma/dt(\uparrow\uparrow)}{\langle d\sigma/dt\rangle}$	$\frac{d\sigma/dt(\downarrow\downarrow)}{\langle d\sigma/dt\rangle}$	$\frac{d\sigma/dt(\uparrow\downarrow)}{\langle d\sigma/dt\rangle}$
0.6	1.8 ± 0.4	1.9 ± 0.5	1.8 ± 0.3	6.7 ± 0.7	1.103 ± 0.009	1.031	0.933 ± 0.007
0.7	0.0 ± 0.4	0.9 ± 0.6	0.4 ± 0.3	5.8 ± 0.9	1.066 ± 0.011	1.050	0.942 ± 0.009
0.8	2.1 ± 0.5	1.9 ± 0.7	2.0 ± 0.4	3.0 ± 1.1	1.070 ± 0.014	0.990	0.970 ± 0.011
0.9	3.2 ± 0.5	3.2 ± 0.7	3.2 ± 0.4	−1.1 ± 1.1	1.053 ± 0.014	0.925	1.011 ± 0.011
1.0	6.0 ± 0.7	8.0 ± 1.0	7.0 ± 0.6	3.9 ± 1.7	1.179 ± 0.021	0.899	0.961 ± 0.017
1.2	12.6 ± 0.9	16.8 ± 1.2	14.7 ± 0.7	8.4 ± 2.0	1.378 ± 0.024	0.790	0.916 ± 0.020
1.4	15.8 ± 0.8	15.5 ± 1.1	15.7 ± 0.6	8.1 ± 1.6	1.395 ± 0.020	0.767	0.919 ± 0.016
1.6	12.1 ± 1.3	15.5 ± 1.7	13.8 ± 1.0	11.2 ± 2.8	1.388 ± 0.034	0.836	0.888 ± 0.028
1.8	11.1 ± 0.8	11.3 ± 1.1	11.2 ± 0.7	10.9 ± 1.7	1.333 ± 0.022	0.885	0.891 ± 0.017
2.2	6.9 ± 1.2	6.0 ± 1.5	6.4 ± 1.0	7.3 ± 2.4	1.201 ± 0.031	0.945	0.927 ± 0.024

* All errors are statistical. There are additional normalization uncertainties due to our knowledge of P_B and P_T which typically total ± 0.5%.

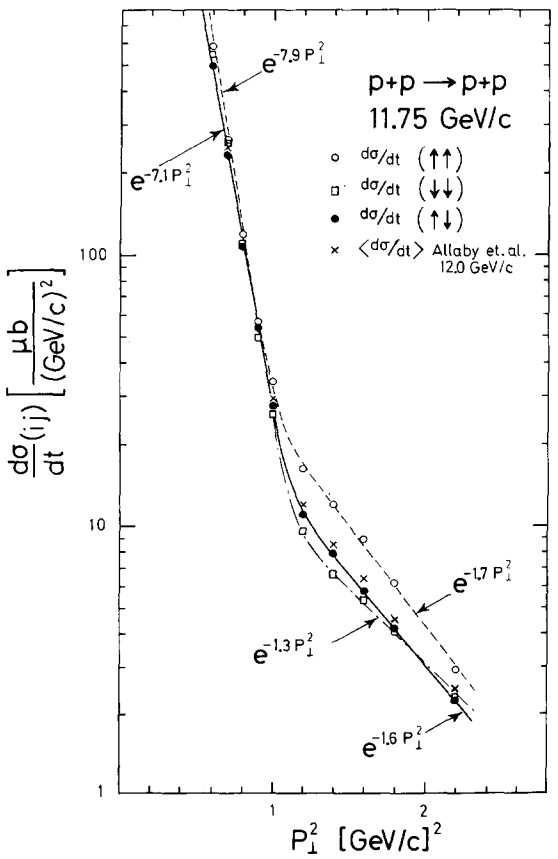

The equality of A_B and A_T required by rotational invariance gave a consistency check which held to within the errors for each $P_\perp^2$ point as shown in table 1. By averaging A_B and A_T we obtained an even more precise value of A.

The differential cross sections obtained from this data are plotted in fig. 2 as $d\sigma/dt(ij)$ against $P_\perp^2$. The $d\sigma/dt(ij)$ are normalized to the 12.0 GeV/c measurements of $\langle d\sigma/dt\rangle$ of Allaby et al. [13], who quote a ±15% normalization error and a ±8% point to point error. These errors do not affect the comparison between the different spin states at each $P_\perp^2$ which have 1 or 2% errors not visible on this plot.

The most striking feature of this graph is the sharp change in the spin dependence at the break in the cross section. In the small $P_\perp^2$ diffraction peak, all three $d\sigma/dt(ij)$ drop off rapidly as $\exp(-7.1\ P_\perp^2)$ to $\exp(-7.9\ P_\perp^2)$. The diffraction peak spin dependence is fairly difficult to see on this graph, however, $d\sigma/dt(\uparrow\downarrow)$ clearly crosses $d\sigma/dt(\downarrow\downarrow)$ at about $P_\perp^2 = 0.8$ (GeV/c)^2. There is then a sharp break in $d\sigma/dt(\uparrow\uparrow)$ at $P_\perp^2 \approx 1.0$ (GeV/c)^2 while $d\sigma/dt(\uparrow\downarrow)$ and $d\sigma/dt(\downarrow\downarrow)$

Fig. 2. The differential elastic proton proton cross sections, $d\sigma/dt(ij)$, for each pure initial spin state are plotted against $P_\perp^2$ at 11.75 GeV/c. The initial spins (i, j = beam, target) are measured normal to the scattering plane and the forward proton scatters to the left as shown in fig. 1. The errors shown are for the spin dependence only and there are additional 8% and 15% normalization errors in $\langle d\sigma/dt\rangle$ described in the text [13].

do not break until about $P_\perp^2 \approx 1.1$ (GeV/c)^2. After the breaks, $d\sigma/dt(\uparrow\uparrow)$ and $d\sigma/dt(\uparrow\downarrow)$ have roughly similar slopes: $\exp(-1.7\,P_\perp^2)$ and $\exp(-1.6\,P_\perp^2)$ respectively, and $d\sigma/dt(\uparrow\uparrow)$ is some 50% larger than $d\sigma/dt(\uparrow\downarrow)$. Notice that $d\sigma/dt(\downarrow\downarrow)$ starts off in this large $P_\perp^2$ region being smallest but has a much flatter slope, $\exp(-1.3\,P_\perp^2)$. It crosses $d\sigma/dt(\uparrow\downarrow)$ at about $P_\perp^2 \approx 1.8$ (GeV/c)^2 and seems to be heading towards $d\sigma/dt(\uparrow\uparrow)$. We plan to see if this behavior continues at larger $P_\perp^2$.

It is interesting that the break in each pure spin cross section is quite sharp. These breaks occur at a different $P_\perp^2$ for each $d\sigma/dt(ij)$ which may cause smoothing in $\langle d\sigma/dt\rangle$. It would be interesting to study these pure spin cross sections at very high energy where $\langle d\sigma/dt\rangle$ itself has a sharp dip at the end of the diffraction peak [14]. The behavior of the $d\sigma/dt(ij)$ may give some indication about the source of this dip. In a geometrical model, the inequality of the slopes and the magnitudes of the different $d\sigma/dt(ij)$ indicates that the proton proton interaction regions have different sizes for each different spin state [15].

The values of A and C_{nn} at 11.75 GeV/c obtained from the data are listed in table 1 and plotted against $P_\perp^2$ in fig. 3 along with other data. Our results generally agree well with other measurements of A near 12 GeV/c [2, 12, 16] but are more precise. There are no previous measurements of C_{nn} near 12 GeV/c. We have also plotted our earlier measurements of A and C_{nn} at 6 GeV/c [6, 7] to observe the energy dependence of these Wolfenstein parameters.

The general behavior of A was known from earlier experiments [2, 12, 16, 17] and our new more precise measurements only emphasize it. In the diffraction peak region A decreases rapidly with energy and is typically 5% near 12 GeV/c. In the large angle region beyond $P_\perp^2 = 1$ (GeV/c)^2 A is quite large, typically 15%, and appears approximately independent of energy. Near $P_\perp^2 = 0.7$ (GeV/c)^2 A has a minimum at 6 GeV/c which becomes a narrow zero at 11.75 GeV/c. Our tiny errors make this zero very clear.

The behavior of C_{nn} is quite surprising. At 6 GeV/c C_{nn} is about 10% in the diffraction peak but drops to about 3% at large $P_\perp^2$ and has little structure. At 11.75 GeV/c C_{nn} has a very narrow dramatic zero which occurs at $P_\perp^2 = 0.9$ (GeV/c)^2 and is somewhat similar to the zero in A. The similarity of these narrow structures in A and C_{nn} suggest looking for some relation between them, but we could find no obvious relation from general principles.

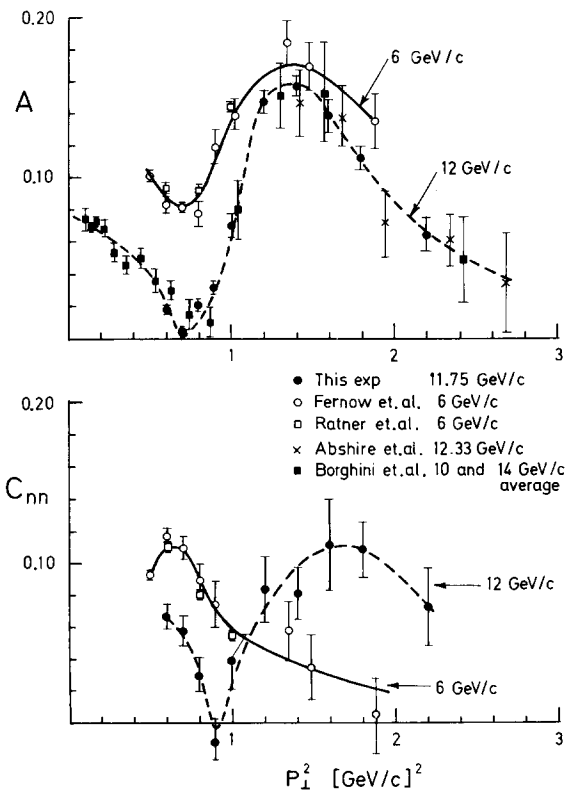

Fig. 3. The Wolfenstein parameters A and C_{nn} for p–p elastic scattering near 6 and 12 GeV/c are plotted against $P_\perp^2$. For some other experiments [2, 6, 12, 16] some bin sizes have been increased at large $P_\perp^2$ to improve the statistical error. A few points with very large errors have been ignored. The curves are hand-drawn lines to guide the eye.

At large $P_\perp^2$, C_{nn} has a broad maximum and is much larger at 11.75 GeV/c than at 6 GeV/c. This large $P_\perp^2$ behavior is quite interesting as it was not expected that the spin dependence of strong interactions would increase with increasing energy. Our data indicates that at large $P_\perp^2$ the spin-orbit interaction ‡ A is rather independent of energy, while the spin-spin interaction, C_{nn}, seems to increase with energy between 6 and 12 GeV/c.

‡ The left-right asymmetry, A, parametrizes the spin-orbit interaction, for it measures that part of $d\sigma/dt$ which depends on the spins being parallel or antiparallel to the orbital angular momentum. Similarly C_{nn} parametrizes the spin-spin interaction, for it measures the difference between the spin-parallel and spin-antiparallel cross sections.

We are very grateful to the ZGS staff for the successful operation of the 11.75 GeV/c polarized beam and for their help with PPT V and our other apparatus.

References

[1] P. Grannis et al., Phys. Rev. 148 (1966) 1297.
[2] M. Borghini et al., Phys. Lett. 24B (1967) 77; 31B (1970) 405; 36B (1971) 501;
M.G. Albrow et al., Nucl. Phys. B23 (1970) 445.
[3] N.E. Booth et al., Phys. Rev. Lett. 21 (1968) 651; 23 (1969) 192; 25 (1970) 898; Phys. Rev. D8 (1973) 45.
[4] E.F. Parker et al., Phys. Rev. Lett. 31 (1973) 783; 32 (1974) 77; 34 (1975) 558.
[5] G. Hicks et al., Phys. Rev. D12 (1975) 2594.
[6] R.C. Fernow et al., Phys. Lett. 52B (1974) 243.
[7] L.G. Ratner et al., to be published. Measurement of 6 GeV/c p-p 3-spin cross sections.
[8] T.K. Khoe et al., Particle Accelerators 6 (1975) 213.
[9] Y.C. Cho et al., private communication.
[10] J.A. Bywater et al., ANL internal report;
H.E.T. Miettinen, thesis, Univ. of Michigan (1975).
[11] M. Borghini et al., CERN internal report, He^3 PPT Operation.
[12] G.W. Bryant et al., contribution G1-27 to 1975 Palermo European Phys. Soc. Conf.
[13] J. Allaby et al., Nucl. Phys. B52 (1973) 316.
[14] N. Kwak et al., Phys. Lett. 58B (1975) 283;
C.W. Akerlof et al., Phys. Lett. 59B (1975) 197.
[15] A.D. Krisch, Phys. Rev. 135 (1964) B1456; Phys. Rev. Lett. 19 (1967) 1149.
[16] G.W. Abshire et al., Phys. Rev. Lett. 32 (1974) 1261; Phys. Lett. 58B (1975) 114.
[17] M. Poulet et al., private communication.